Modification of MARS-KS motion model to extend the multi-dimensional flow analysis capability under ocean condition

Hyungjoo Seo, Geon-Woo Kim, Hyoung Kyu Cho
Department of Nuclear Engineering, Seoul National Univ., 1 Gwanak-ro, Gwanak-gu, Seoul 08826
[*]Corresponding author: chohk@snu.ac.kr

1. Introduction

As various countries have a spotlight on the nuclear energy as a power for the commercial ship propulsion and the floating power plant, several domestic institutions are developing the marine reactors [1, 2]. They have distinct hydrodynamic features from those of land-based reactors as they operate in the motion. Therefore, the advanced safety analysis code is required to evaluate the performance of the reactor by modeling external motion effects on the thermal-hydraulic phenomena. The ultimate goal of the code is to develop and verify the physical models under motion conditions, however, improving the governing equations must be preceded first. In the previous studies, the dynamic motion model was implemented in MARS-KS [3] by modeling external forces for dynamic motion in the momentum equations. Specifically, Beom et al. [4] modified the input option for the arbitrary motion and determination procedure of the flow regime map under motion condition. Subsequently, Beom et al. [5] and Park et al. [6, 7] revised the cross-flow model by generalizing the concept of the junction connection and showed the possibility that the motion model can also work in the MULTID component.

Nevertheless, the applicability of the motion model is still restricted in MULTID components. In order to analyze the three-dimensional flow behaviors in the reactor vessel or the steam generator of the marine reactor, the motion model should be extended for the MULTID components. Therefore, in this study, the calculation of the pressure in the junctions was modified to reduce the numerical errors. Then, the Coriolis force was modeled in the momentum equations for MULTID component allowing the simulation of the multi-dimensional flow affected by dynamic motion. Followed modifications were verified or tested with the conceptual problems consisting of the MULTID component under rotating conditions.

2. Modification of MARS-KS motion model for MULTID component

In this section, two main modifications of the code will be discussed to extend the motion model for MULTID components. Firstly, the formula for calculating the pressure head was improved to have better accuracy. Secondly, Coriolis force was also modeled considering the multi-dimensional effect. The modified code has been verified with the conceptual problems.

2.1. Pressure head calculation with enhanced accuracy

The dynamic motion makes the additional acceleration including the frame acceleration, centrifugal acceleration, tangential acceleration and Coriolis acceleration. They can be arranged into the total acceleration ($\overrightarrow{\boldsymbol{a_{tot}}}$) as:

$$a_{tot,x} = x\left(\omega_y{}^2 + \omega_z{}^2\right) + y\left(-\omega_x\omega_y + \beta_z\right) + z\left(-\omega_x\omega_z - \beta_y\right) - a_{cor,x} - a_{tran,x} \quad (1)$$

$$a_{tot,y} = y(\omega_x{}^2 + \omega_z{}^2) + x\left(-\omega_x\omega_y - \beta_z\right) + z\left(-\omega_y\omega_z + \beta_x\right) - a_{cor,y} - a_{tran,y} \quad (2)$$

$$a_{tot,z} = z\left(\omega_x{}^2 + \omega_y{}^2\right) + x\left(-\omega_x\omega_z + \beta_y\right) + y(-\omega_y\omega_z - \beta_x) - a_{cor,z} - a_{tran,z} - g \quad (3)$$

where $\vec{\boldsymbol{R}} = (x, y, z)$ is a position vector of the volume, $\vec{\boldsymbol{\omega}} = (\omega_x, \omega_y, \omega_z)$ is a angular velocity vector, $\vec{\boldsymbol{\beta}} = (\beta_x, \beta_y, \beta_z)$ is a angular acceleration vector, $\overrightarrow{\boldsymbol{a_{cor}}}$ is a Coriolis acceleration vector, $\overrightarrow{\boldsymbol{a_{tran}}}$ is a translational acceleration vector, and g is the gravity.

These accelerations generate the extra pressure head in the momentum equations. Supposing the volume K and L are connected with a junction, it can be analytically derived in integral form as Eq. (4) where ρ is a density and $\vec{\boldsymbol{H}}$ is a volume connection vector.

$$\Delta P(K \to L) = \int_K^L \rho \overrightarrow{\boldsymbol{a_{tot}}} \cdot \overrightarrow{\boldsymbol{dH}} = \int_K^L \rho a_{tot,x} dx + \int_K^L \rho a_{tot,y} dy + \int_K^L \rho a_{tot,z} dz \quad (4)$$

From Eq. (1)~(3), the total acceleration in each axis can be interpreted as a linear function of x, y, and z respectively. For example, the theoretical calculation of integrals along the x-axis appears as Fig. 1-(a) where *f(x)* is a function of the density times the total acceleration. However, it was found that the existing motion model had bad accuracy in calculating integrals in some conditions. This is because MARS-KS took a numerical scheme of the rectangular sum integration in the pressure head calculation as Eq. (5) and Fig. 1-(b). It could generate the truncation errors when connected volumes have different size or density.

$$\int_K^L \rho a_{tot,x} dx = \rho_K a_K H_K + \rho_L a_L H_L \quad (5)$$

Since the MULTID component often consists of the different sized volumes or multi-phase flow, it is important to enhance the accuracy of computing pressure in the motion model for MULTID component. Thus, the integration formula has been modified as shown in Eq. (6) using the constant *S* which is a slope of *f(x)*.

$$\int_K^L \rho a_{tot,x} dx = \frac{1}{2}\rho_K H_K(2a_K + S_K H_K) + \frac{1}{2}\rho_L H_L(2a_L - S_L H_L) \qquad (6)$$

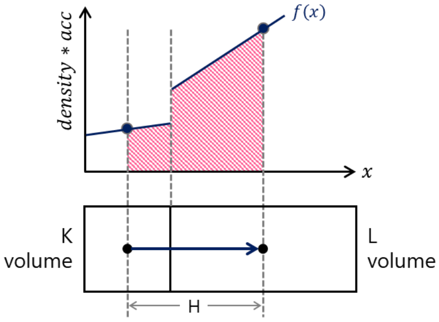

(a)

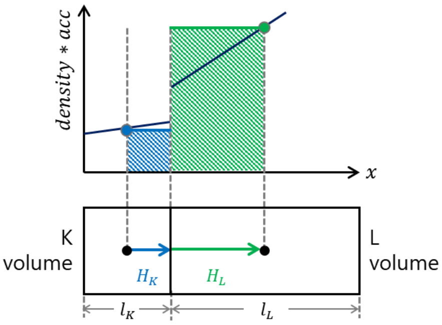

(b)

Fig. 1. Pressure head calculation between two connected volumes with (a) analytical integration (b) rectangular sum integration

2.2. Verification of the pressure calculation

The rectangular slab problem in Fig. 2-(a) was selected to verify the pressure calculation in the modified code. In this conceptual problem, the slab rotates on the z-axis with constant speed of 120°/s under zero gravity condition.

The simulations were conducted for the single-phase (Case 1) and the two-phase (Case 2) conditions using two kinds of meshes. Mesh A and B in Fig. 2-(b) have a different size of the grid, but the colored volumes are in the identical positions. Therefore, the pressure difference between them should be same.

The calculated pressure differences are shown in Fig. 3 and 4. In the both cases, there were disagreement in the results before the modification. However, the modified code showed consistent results within 0.2% no matter which mesh it used. It also calculated the same void fraction distribution in the slab for the both meshes as shown in Fig. 4-(c).

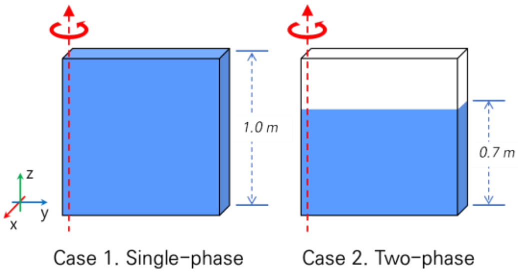

(a)

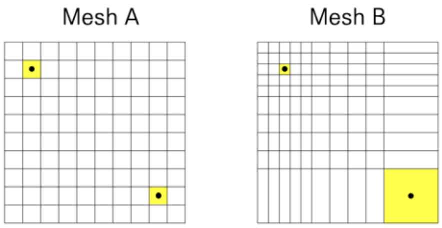

(b)

Fig. 2. Conceptual problem of rotating rectangular slab (a) Geometry (b) Mesh configuration

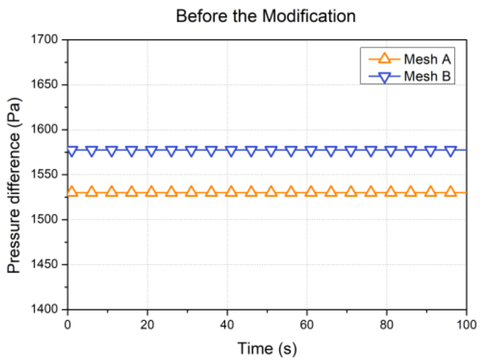

(a)

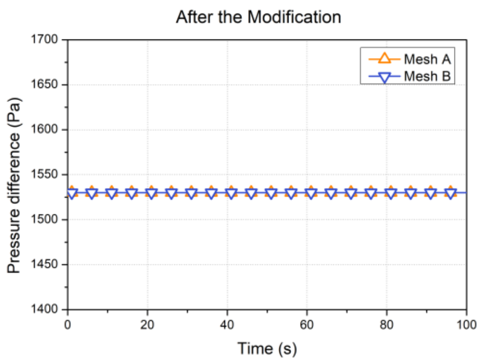

(b)

Fig. 3. Simulation results of Case 1 (a) before modification (b) after modification

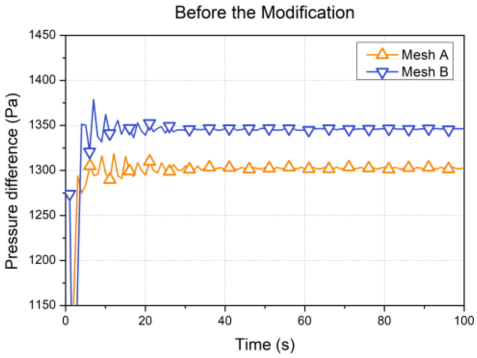

(a)

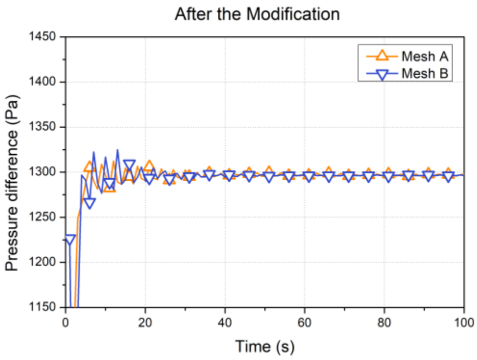

(b)

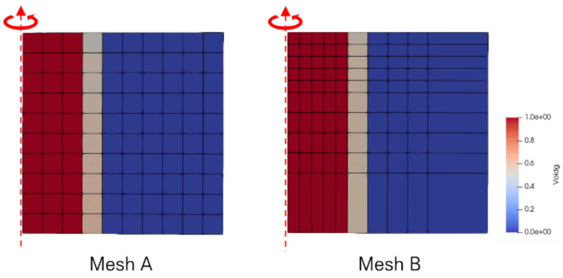

(c)

Fig. 4. Simulation results of Case 2 (a) before modification (b) after modification (c) void fraction distribution result from the modified code

2.3 Coriolis force

The Coriolis force is a fictitious force that appears when the frame of reference rotates. By definition, its direction is always perpendicular to the rotation axis and the flow direction. In previous model, it has been neglected because the model was developed focusing on one-dimensional momentum equation. However, to demonstrate the effect of dynamic motion on fluid flow in MULTID component, the momentum equation should be modified by modeling the Coriolis force as an additional acceleration term.

The governing equation in MARS-KS is a sum of differential momentum equations for liquid and vapor phases. The external body force by the dynamic motion is also modeled in a form of summing the forces in each phase. It is determined from the acceleration and the mixture density in Eq. (7). Thus, the Coriolis acceleration should be defined considering the calculation with the density as expressed in Eq. (8).

$$\rho_m = \alpha_g \rho_g + \alpha_f \rho_f \tag{7}$$

$$\rho_m \overrightarrow{\boldsymbol{a_{cor}}} = \rho_m \left[\frac{\alpha_g \rho_g}{\rho_m} \left(2\overrightarrow{\boldsymbol{\Omega}} \times \overrightarrow{\boldsymbol{v_g}} \right) + \frac{\alpha_f \rho_f}{\rho_m} \left(2\overrightarrow{\boldsymbol{\Omega}} \times \overrightarrow{\boldsymbol{v_f}} \right) \right] \tag{8}$$

2.4 Verification of the Coriolis force

Y channel problem described in Fig. 5 was simulated to verify the effect of the Coriolis force in the modified code. It contains the channels modeled with the MULTID component, and the water constantly flows through the inlets while the channel rotates on the z-axis. Since it is complex to derive the analytical solution for the Coriolis force, the simulation results of the problem have been qualitatively analyzed. It can be expected that the flow in the channel 2 will increase because of the Coriolis force as described in Fig. 5.

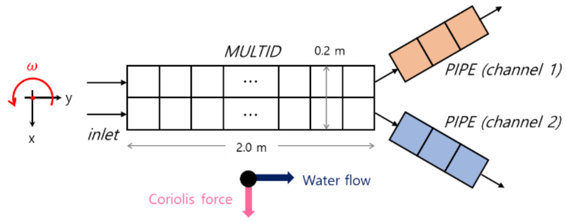

Fig. 5. Conceptual problem of Y channel

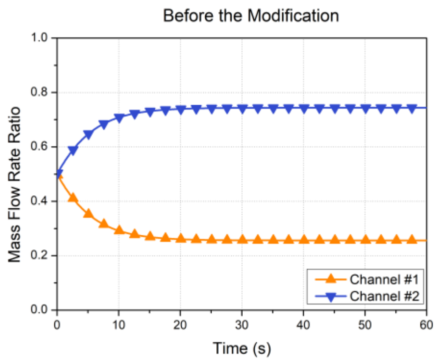

(a)

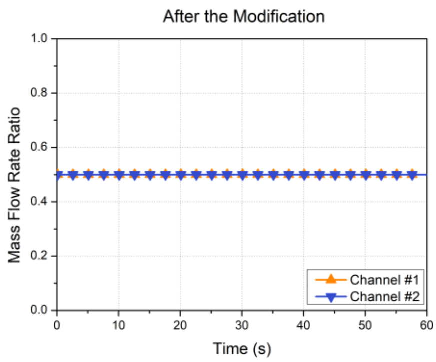

(b)

Fig. 6. Mass flow rate ratio at the outlets ($\omega = 10°/s, v_{in} = 0.05 m/s$) (a) before modification (b) after modification

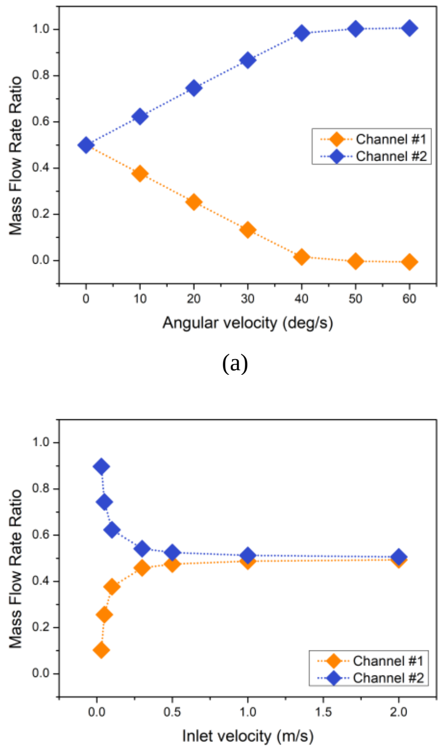

(a)

(b)

Fig. 7. Mass flow rate ratio according to (a) angular velocity ($v_{in} = 2.0m/s$) (b) inlet velocity ($\omega = 10°/s$)

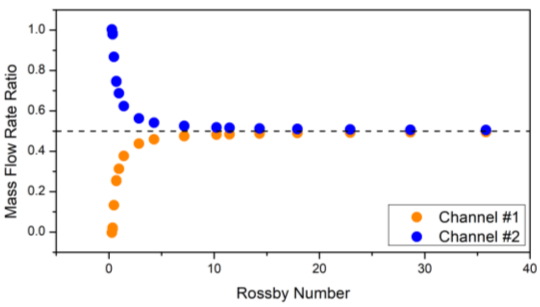

Fig. 8. Mass flow rate ratio according to Rossby number

Figure 6 shows the calculation results of the mass flow rate ratio in each channel which is normalized by the inlet mass flow rate. The modified code calculated the bigger mass flow in the channel 2 due to the Coriolis force acting in the positive x direction as expected, whereas this effect did not show up in the result without the modification.

In addition, the following parametric effects were tested. The Coriolis force increased as the Y channel rotated with faster angular velocity under the fixed inlet velocity. The asymmetric flow in two outlets became severe (Fig. 7-(a)). On the other hand, when the inlet velocity increased with constant rotating speed, the effect of Coriolis force weakened (Fig. 7-(b)).

This parametric effect of Coriolis force also can be described with Rossby number in Eq. (9):

$$\mathrm{Ro} = \frac{Inertial\ force}{Coriolis\ force} = \frac{U}{hf} \tag{9}$$

where *U* and *h* is a characteristic velocity and length, and *f* is a Coriolis frequency. Figure 8 shows the mass flow rate in the channels with Rossby number. As Rossby number increased, the flow inertia force became dominant rather than the Coriolis force. Then it makes the mass flow in two channels become similar. The difference between two mass flow rate ratios was under 3.5% if the Rossby number is above 10. Assuming the marine reactor under ocean conditions, the Rossby number is found to be bigger than a few ten. Therefore, it is expected that the Coriolis force will not be significant in the reactor.

3. Conclusions

In the present work, the dynamic motion model of MARS-KS has been improved with two code modifications to extend its capability in MULTID component. First, to enhance the accuracy in calculating the pressure head by the acceleration, the numerical scheme for computing the integrals has been modified. The slab conceptual problem verified the improved formula worked for any volume conditions. Second, the Coriolis force was newly added in the governing equations of the MULTID component. In the Y channel problem, the asymmetric flow appeared as a result of the Coriolis force after the code modification. Rossby number can describe the Coriolis effect compared to the flow inertia. In future works, it is necessary to verify the Coriolis force model quantitatively.

In this study, the extended model enables MARS-KS to analyze the multi-dimensional flow in the marine reactors on a fundamental level. However, the dynamic motion model has a number of things to be improved further including the models for special components or processes in the system code. Moreover, various physical models for thermal-hydraulics under the dynamic condition should be developed by experimental studies in the future.

ACKNOWLEDGEMENT

This work was supported by the Nuclear Safety Research Program through the Korea Foundation Of Nuclear Safety(KoFONS) using the financial resource granted by the Nuclear Safety and Security Commission(NSSC) of the Republic of Korea. (No. 2003005)

REFERENCES

[1] I.H. Kim, J.S. Won, T.H. Bae et al., Development of BANDI-60S for a floating nuclear power plant, Transactions of the Korean Nuclear Society Autumn Meeting, Goyang, Korea, Oct. 24-25, 2019.

[2] D.K. Kim, B.S. Oh, J.I. Lee, Control logic development of KAIST Micro Modular Reactor for marine propulsion,

Transactions of the Korean Nuclear Society Spring Meeting, Jeju, Korea, May 18-19, 2017.
[3] J. J. Jeong, K. S. Ha, B. D. Chung, W. J. Lee., Development of a multi-dimensional thermal-hydraulic system code, MARS 1.3.1, Annals of Nuclear Energy, 26, pp. 1611-1642, 1999.
[4] H.K. Beom, G.W. Kim, G.C. Park, H.K. Cho, Verification and improvement of dynamic motion model in MARS for marine reactor thermal-hydraulic analysis under ocean condition, Nuclear Engineering and Technology, 51, pp.1231-1240, 2019.
[5] H.K. Beom, G.W. Kim, G.C. Park, H.K. Cho, Improvement of dynamic motion model in MARS-KS for downcomer modeling of a maritime reactor with cross-junction connection, Transactions of the Korean Nuclear Society Spring Meeting, Jeju, Korea, May 23-24, 2019.
[6] S.W. Park, G.W. Kim, H.K. Cho, Status of MARS-KS modification for thermal-hydraulic analysis of a marine reactor, Korean Society for Fluid Machinery Summer Conference, Pyeongchang, Korea, Aug. 24-26, 2020.
[7] S.W. Park, H.J. Seo, H.K. Cho, Extension of MARS-KS motion model to MULTID component modifying volume connection information for marine reactor simulation, Transactions of the Korean Nuclear Society Autumn Meeting, Changwon, Korea, Oct. 22-23, 2020.